Excitation and Temperature Stability of PCB Fluxgate Sensor

Alois Tipek, Terence O'Donnell, *Member, IEEE*, Pavel Ripka, *Fellow, IEEE*, and Jan Kubik

***Abstract*—Printed circuit board (PCB) integrated inductors have been adapted for operation as fluxgate sensors. A ring core is made from an electrodeposited permalloy thin film and is sandwiched between the layers of the PCB. The sensor excitation winding is also integrated into the PCB design. The pick-up coil is wound around the frame of the PCB core. Different types of current excitation waveforms with tuned and nontuned pick-up coils were used. The achieved sensitivities for 60 turns of tuned/nontuned pick-up coil, a sinusoidal waveform excitation current of $\mathrm{Irms} = 300$ mA, and an excitation frequency of 150 kHz were 13100/1800 V/T. The achieved sensitivity for pulse excitation ($\mathrm{Ipeak\text{-}peak} = 900$ mA, $\mathrm{Irms} = 184$ mA, duty 20%) was 2100 V/T. Noise power density for pulse excitation was 1.2 nTrms/$\sqrt{\text{Hz}}$@1 Hz, noise rms value from 10 mHz to 10 Hz was 3.3 nT. A perming error of 1 μT was measured for a wide range of excitation currents.**

***Index Terms*—Excitation, fluxgate sensor, printed circuit board (PCB), temperature stability.**

I. Introduction

THE fluxgate sensor is one of the most popular precise magnetic field sensors but the complicated construction of the core and coils present an obstacle for reducing the production price [1] and the size. Several research groups have been seeking solutions for reducing the size and cost of fluxgate sensors using standard planar technology [2]–[5] and PCB technology [6]–[9]. Fluxgate mode can also be used in AMR sensors [10].

The sensor presented here was adapted from previously developed PCB-integrated inductors [11]. The main objective of our work is to develop a cheap fluxgate sensor technology based on embedding magnetic materials inside multilayer printed circuit boards (PCBs). This paper describes the performance of a PCB technology fluxgate sensor measured using different types of excitation current waveform and for tuned and nontuned pick-up coils. In previous work, the authors proved the functionality of the sensor but the main disadvantage of the construction was the power consumption caused by the sine wave excitation [12]. In this work, a pulse waveform excitation current has been used to reduce RMS value of the excitation current, and, hence, the power dissipation. The performance of the sensor is measured using this pulse waveform and is compared to the performance with sinusoidal excitation. The temperature stability of the sensor offset and sensitivity is also investigated.

Manuscript received February 4, 2004; revised October 29, 2004. This work was supported in part by the Irish Research Council for Science (IRCSET) under Embark Initiative Grant PD2002/52 and in part by the Ministry of Education (FRVS) of the Czech Republic under Grant 2474/2003. The associate editor coordinating the review of this paper and approving it for publication was Dr. Subhas Mukhopadhyay.

A. Tipek and T. O'Donnell are with the Tyndall National Institute, Cork, Ireland (e-mail: atipek@tyndall.ie; terence.odonnell@tyndall.ie).

P. Ripka and J. Kubik are with the Department of Measurement, Czech Technical University, Prague, Czech Republic (e-mail: ripka@feld.cvut.cz; jan.kubik@centrum.cz).

Digital Object Identifier 10.1109/JSEN.2005.859239

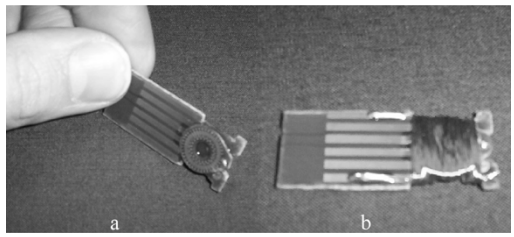

Fig. 1. Image of the PCB integrated fluxgate sensor. (a) Before the pickup coil has been wound. (b) With pickup coil.

II. Sensor Construction

The construction is derived from the inductor embedded in PCB technology. The magnetic core has the form of two 22-μm-thick toroids made of electrodeposited permalloy, which are embedded between the layers of the PCB. The toroids have an inner diameter of 7 mm and an outer diameter of 10 mm. The sensor excitation winding is also integrated into the PCB design: individual conductor sections in the lower and upper copper layers are connected by vias, thus forming 40 turns with a total resistance of 700 mΩ,which encircle the magnetic core. For an excitation current of 1 A, a magnetic field intensity of 1.45 kA/m $=$ 18 Oe is created in the core [13]. Fig. 1(a) shows the PCB with the embedded magnetic core and the excitation winding. The pick-up coil of the fluxgate sensor was implemented using an external winding with 0.2 mm diameter copper wire. In order to wind the pickup coil, the PCB core was mounted on a frame made from a second PCB (as shown in Fig. 1(a) and the 60 turns pickup coil was wound around this frame. Fig. 1(b) shows the sensor with the pickup coil.

III. Sensor Excitation

A. Sinusoidal Excitation

The simplest fluxgate sensor excitation with a sinusoidal current was implemented and presented in [12]. The initial testing was performed with an un-tuned pick-up coil. Later the pick-up coil was tuned to have a resonance at 300 kHz by using a parallel 10 nF capacitor. Fig. 2 shows the traces of the excitation current and pick-up coil voltage for the sinewave excitation. The sensitivities achieved for a tuned and un-tuned pick-up coil were 13 100 and 1800 V/T, respectively, for an rms excitation current

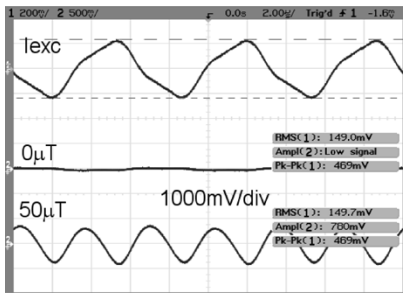

Fig. 2. Sinewave excitation $f = 150$ kHz and tuned pick-up coil Cp $= 10$ nF [11] The top trace is the excitation current (400 mA/div). The middle trace is the pick-up coil voltage for zero external field $B = 0$ μT. The bottom trace is the pick-up coil voltage for $B = 50$ μT.

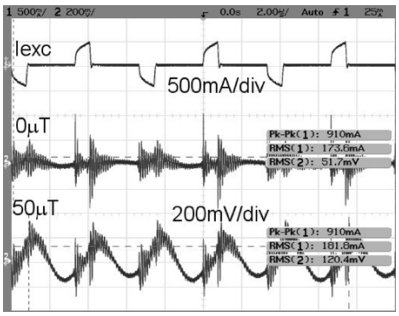

Fig. 3. Pulse excitation $f = 150$ kHz and duty 20% tuned pick-up coil Cp $=$ 10 nF. The top trace is the excitation current (500 mA/div). The middle trace is the pick-up coil voltage for zero external field $B = 0$ μT. The bottom trace is the pick-up coil voltage for $B = 50$ μT.

of 300 mA [12]. The noise power density for tuned pick-up coil was 200 pT/$\sqrt{\text{Hz}}$@1 Hz and the noise rms level was 0.3 nT in the frequency range 10 mHz to 10 Hz. The perming error (shock field sensitivity) was 0.5 μT for a shock field of 10 mT [12]. Resonance of the excitation coil could not be achieved due to its high resistance and relatively low inductance.

B. Pulse Excitation

The rms value of the excitation current, and, hence, the power dissipation of the sensor can be reduced by using pulse excitation. Fig. 3 shows the traces of excitation current and pick-up coil voltage for the pulse waveform excitation. The design of the excitation electronics was described in [14]. In this case, the pick-up coil is tuned with a parallel 10 nF capacitor. The peak–peak value of the excitation current in both Figs. 2 and 3 is $I_{p\text{-}p} = 900$ mA, at an excitation frequency of 150 kHz. The duty cycle for pulse excitation was 20%; therefore, the rms value of the current was only 184 mA (sinewave 300 mA).

In Sections V and VI, the characteristics of the sensor using the pulse excitation are measured and the temperature stability of the sensor is investigated. These new investigations continue and extend the previous work on the PCB fluxgate, which has been summarized above. To the authors knowledge, this is the first time that the temperature sensitivity of a PCB embedded fluxgate sensor has been presented.

IV. Test Results

A digital lock-in amplifier (Stanford Research SR 844) was used for measurement of the sensor characteristics. The reference was set to second harmonic and the phase was always adjusted for maximum sensitivity. The computer controlled measurement system was driven by LabVIEW software. An external magnetic field was applied by placing the sensor in a Helmholtz coil system. The value of the Earth's field was subtracted from the Helmholtz coil field during the data processing.

A. Sensitivity

Fig. 4 shows the second harmonic of the sensor pickup voltage versus the applied magnetic field for field values in the range of the earth's field. The sensor characteristic is shown for various values of the excitation current. In this case the pick-up coil is tuned by a parallel capacitor Cp $=$ 10 nF. The pulse excitation duty is 20% in all cases. As can be seen, the sensor characteristics are linear and the sensor sensitivity is increasing with excitation current amplitude.

Fig. 5 plots the sensor sensitivity versus the excitation current. This figure shows that the sensitivity increases until the excitation current reaches a value of 1800-mA peak–peak. Higher values of the current will not significantly increase the sensitivity, as the PCB core is deeply saturated. However, in general, fluxgate noise and perming effect decrease with increasing excitation amplitude. The optimum performance from the point of view of decreasing noise and perming is usually obtained for excitation levels higher than that which gives maximum sensitivity.

Fig. 6 compares the sensor response for three different sensor configurations over a wide field range. The figure shows how the sensitivity is dependent on the type of the excitation current and whether the pickup coil is tuned or un-tuned. In all cases the excitation frequency is 150 kHz and excitation current peak–peak value is 900 mA. The sensor with the sinewave excitation and the tuned pick-up coil has the highest sensitivity. The lowest sensitivity is for the sinewave current with untuned pick-up coil. The middle sensor response belongs to the pulse excitation with 20% duty and tuned pick-up coil.

The value 900-mA peak–peak was chosen according to the previous sinewave testing measurements in [12]. Fig. 6 shows that this value does not saturate the core sufficiently. The sinewave excitation of 900-mA peak–peak corresponds to an rms value 300 mA, and, in this case, the power dissipation caused heating of the sensor. For the pulse excitation the 900-mA peak–peak value corresponds to a significantly reduced rms value 184 mA.

B. Perming Effect

The perming error of the sensor was also investigated. A dc field of 5 mT was applied in one direction and then the sensor response within -80 to 80 μT was measured. Afterwards a 5-mT field of opposite polarity was applied to the sensor and again the sensor response was measured. The sensor was placed with sensitive axis perpendicular to the horizontal component of the Earth's magnetic field. A series of measurements was performed to investigate the influence of the 5 mT perming field of constant value on the sensor with variable excitation current from 500- to 2000-mA peak–peak. The perming error of the device was 1 μT when using excitation currents ranging from 900- to 2000-mA peak–peak. There was no clear dependence of the perming error

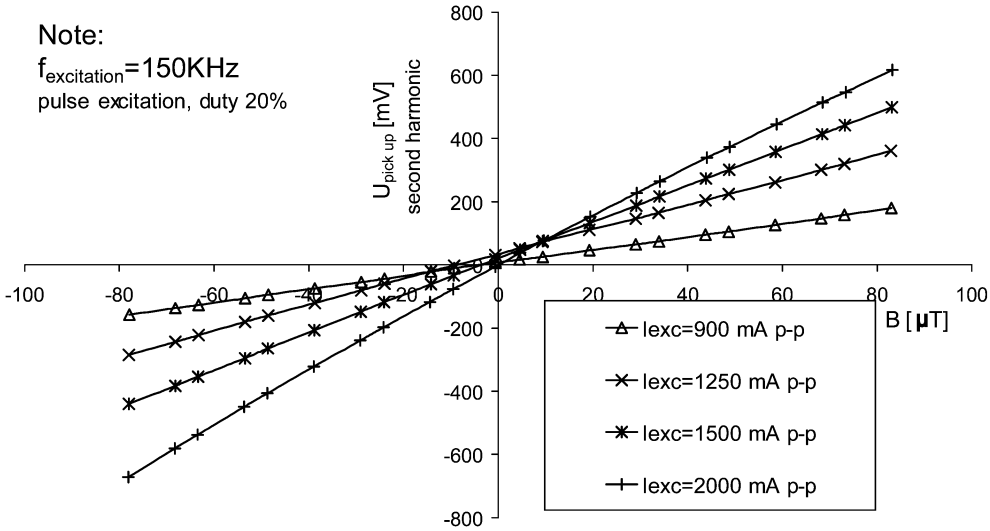

Fig. 4. Second harmonic of the sensor pickup voltage versus applied external field for various excitation currents, using a tuned pick-up coil 10 nF.

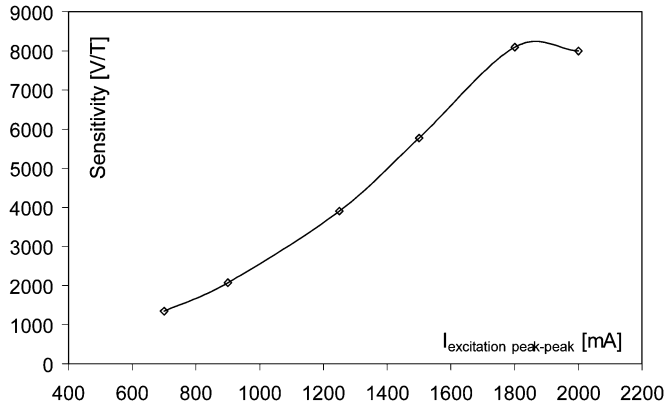

Fig. 5. Sensitivity of the sensor versus peak excitation current.

on the excitation current. This again indicates that the excitation current is too low for full core saturation.

C. Noise

The noise measurements were performed with the sensor placed within a cylindrical enclosure shielded using six layers of permalloy. The Stanford Research SR770 spectrum analyzer and the Agilent 54 621A oscilloscope were used for measurement of the output of the Stanford Research SR844 lock-in amplifier tuned on the second harmonics of the sensor excitation current. The sensor noise characteristics were measured for pulse excitation currents, with an excitation frequency of 150 kHz, a peak–peak current of 900 mA and a tuned pick-up coil (Cp $=$ 10 nF).

Fig. 7 shows the noise power density spectrum for the sensor. The $1/f$ noise shape typical for fluxgate sensors can be seen. The noise value at 1 Hz is 1.2 nTrms/$\sqrt{\text{Hz}}$ and the noise rms value is 3.3 nT in the range of 10 mHz to 10 Hz. Fig. 8 shows the time plot of the sensor noise and indicates that the peak–peak level of the noise is 87 mV, which corresponds to 12 nT. For higher levels of the excitation amplitude the noise level decreases: for 1500 $\text{mA}_{p\text{-}p}$ (300 mA_{rms}) excitation current the noise power density is 180 pTrms/$\sqrt{\text{Hz}}$@1 Hz.

V. Temperature Characteristics

One of the most important characteristics of any sensor is the stability of the parameters, and, here, we investigate the stability of the sensitivity and offset with temperature.

The PCB sensor was placed inside a thermally isolated chamber. This chamber was situated inside the six-layer permalloy shielding in order to isolate it from external fields. Within the chamber the temperature can be controlled in the range -10 °C to $+80$ °C. The chamber is heated from $+20$ °C to $+80$ °C by the power losses in a resistive winding in the chamber. The chamber is cooled to -10 °C by a tube containing anti-freeze liquid which is wound around the chamber. The anti-freeze liquid is cooled by a freezer and then the liquid is pumped into the tube. As a final step, the chamber is heated again to the starting temperature. Fig. 9 shows the measured offset voltage of the sensor versus temperature. The offset remains within 5 μT over the entire temperature range. The temperature stability of the sensor sensitivity was measured in a similar manner [15]. The temperature was varied from $+20$ °C to $+80$ °C, then to -10 °C and then back to $+20$ °C. Fig. 10 shows the sensitivity change with temperature. The sensitivity changes by approximately 20 V/T/ °C so that the temperature coefficient of sensitivity is approximately 1%/°C.

It is though that the change of the sensor parameters with temperature is partly caused by a change of the permeability of the electrodeposited ferromagnetic material used in the sensor core construction. Another contribution is from the change in shape and dimensions due to the temperature coefficient of expansion of the epoxy layers.

The following tests were performed in order to separately investigate the contribution of the PCB structure and core material to the temperature stability. The temperature stability of the inductance is investigated for an electrodeposited NiFe film core embedded in the PCB structure and a stand-alone electrodeposited NiFe film core. The windings on the PCB embedded core are formed from the PCB tracks and vias which surround the sandwiched core as in the case of the sensor. For the stand alone core, turns of copper wire are wound around the core to

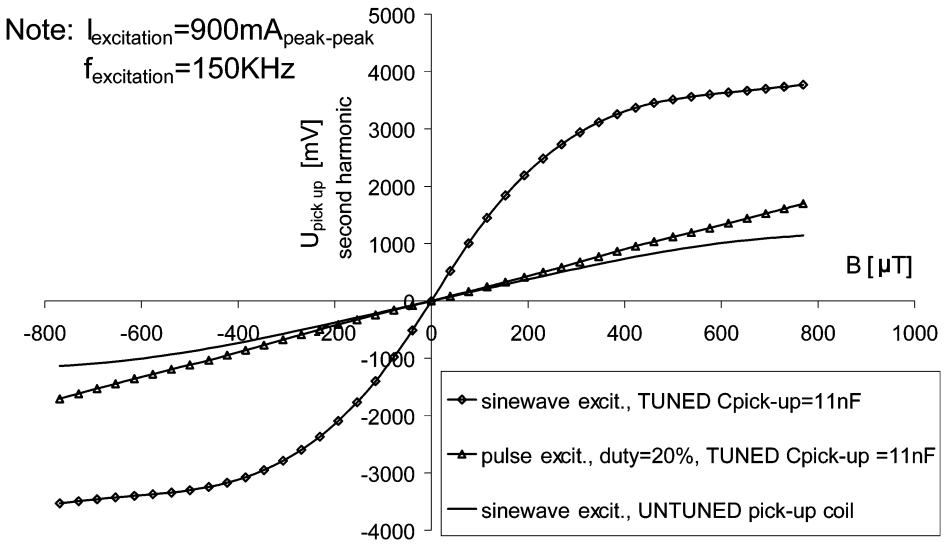

Fig. 6. RMS value of second harmonic pickup voltage vs applied flux density for various excitation schemes.

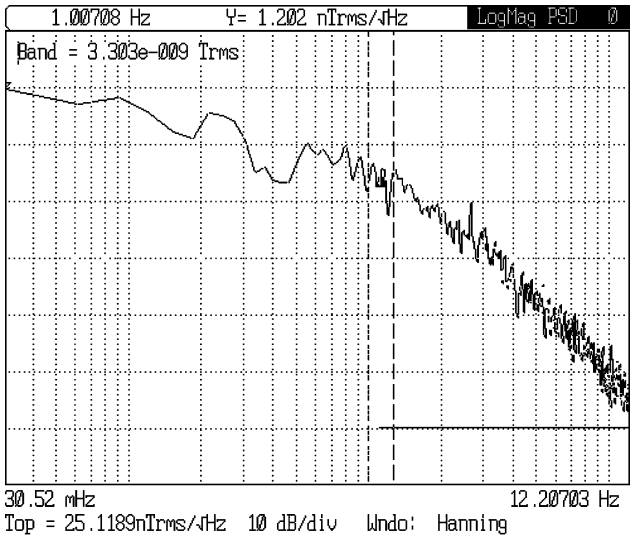

Fig. 7. Sensor noise spectrum for a tuned pick-up coil (Cp = 10 nF), and an excitation frequency, fexc = 150 kHz, excitation current, Iexc = 900 mA$_{p\text{-}p}$, and a pulse duty cycle of 20%.

form a similar inductor. The shape, size and material of the embedded and stand-alone NiFe film cores are the same. These two inductors were slowly heated up to 90 °C and during the heating the inductance value was recorded. Fig. 11 describes change of the inductance in percent for both the embedded and stand-alone core over the temperature change of 60 °C.

The results show that the variation of the inductance for stand-alone NiFe electrodeposited core inductor is in the range less then 5% over 60 °C. The variation of the inductance for the embedded NiFe electrodeposited core inductor is approximately 30% over the same temperature range.

As a conclusion, we would suggest that the major contribution to inductance change versus temperature for the NiFe electrodeposited core inductor is the PCB structure and not the property of NiFe film. This could possibly be explained by the mechanical stress of the core. The core inside PCB structure is stressed by mechanical tension caused by the temperature expansion of PCB layers. The typical expansion factor for a PCB is several 10 s of ppm in the XY plane, but in Z axis, perpendicular to the plane the expansion is approximately 200 ppm. It is, therefore, likely that the temperature stability of the PCB fluxgate sensor is also caused by the mechanical stress imposed on the embedded core and the consequent change in magnetic properties caused by this.

VI. Conclusion

Pulse excitation of a fluxgate sensor using PCB technology was introduced. A 150-kHz 20% duty cycle excitation current was used during testing of the sensor. The pick-up coil tuning capacitor of 10 nF was used for increasing the sensitivity.

The achieved sensitivity was 2100 V/T when using 900-mA peak–peak (184 mA rms) excitation current, but with higher excitation current 1800-mA peak–peak a higher sensitivity of 8100 V/T was experienced. The perming error of the sensor was below 1 μT for 10-mT shock field and excitation currents ranging from 900-mA peak–peak to 2000-mA peak–peak (400-mA rms). The noise power density for 900-mA peak–peak excitation current was 1.2 nTrms/$\sqrt{\text{Hz}}$@1 Hz the noise rms value in range from 10 mHz to 10 Hz was 3.3 nT.

We have shown that pulse excitation could be used in PCB sensor excitation to significantly reduce the consumption, and, therefore, the power dissipation inside the sensor. The power consumption in pulse excitation drops to 60% to equal peak to peak value of the sinewave excitation. The maximum linear range of the sensor also increases due to better saturation of the core. However, the sensor electronics required for pulse excitation is more complicated. Another method which can generally reduce the consumption of the sensor is the use of a resonant circuit with the excitation coil. However, in this case, the excitation coil resistance is high and the inductance is relatively low; therefore, resonance could not be achieved. The resistance could be decreased using thicker PCB tracks but the vias still contribute to the high resistance of the coil. Using bigger vias could improve the resistance but still we are limited with size and space around the core. Other excitation methods, for example using a

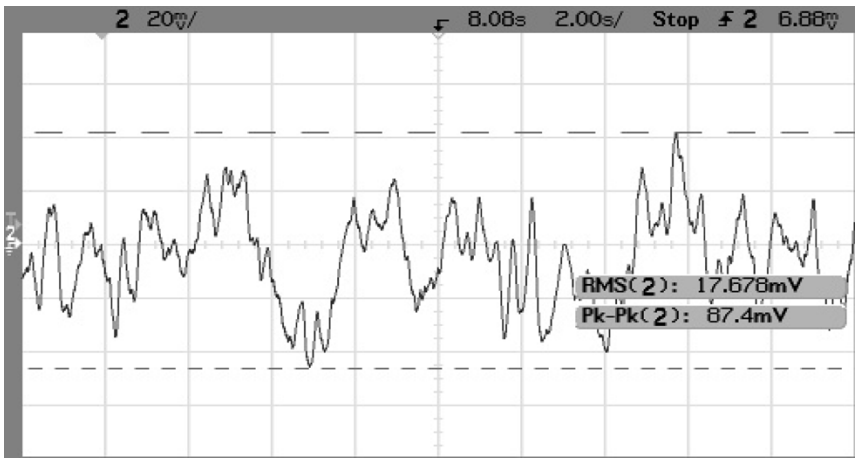

Fig. 8. Sensor noise time plot (2.8 nT/div; 2 s/div).

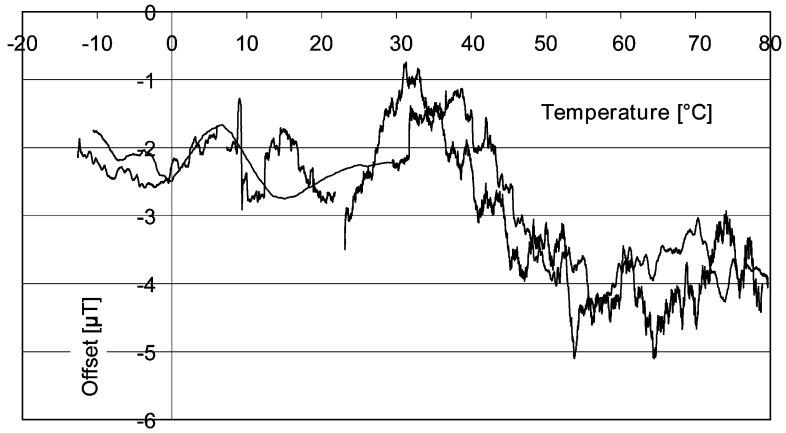

Fig. 9. Offset versus temperature (tun. pick-up coil Cp = 10 nF, fexc = 150 kHz, Iexc = 900 $mA_{p\text{-}p}$, and duty cycle = 20%).

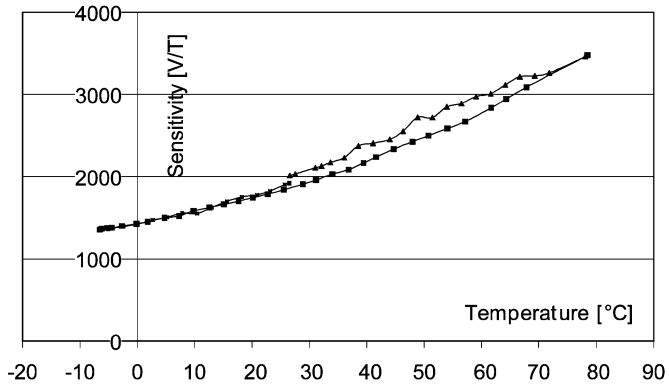

Fig. 10. Sensitivity versus temperature (tuned pick-up coil C = 10 nF, fexc = 150 kHz, Iexc = 900 $mA_{p\text{-}p}$, and duty cycle = 20%).

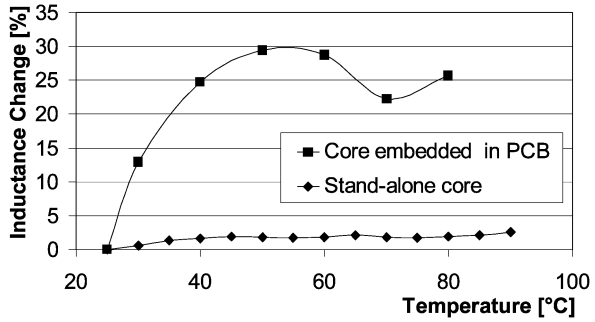

Fig. 11. Inductance change of the sandwiched and stand-alone NiFe cores versus temperature.

saturable inductor in the excitation circuit are currently under development.

A 5-μT offset change was observed for a temperature variation in the range -10 to $+80$ °C and the temperature coefficient of sensitivity was measured to be 1%/°C. The interaction between the core material properties and the thermal expansion of the PCB was investigated. The main contributor to the parameter change with temperature would appear to be stress caused by the PCB structure itself. Therefore, the design of the PCB including the core must be modified, in order to remove the mechanical stress as far as it is possible. Such a modification could include the placement of an air gap between the core and next layer of PCB. The mechanical stress could be also removed by decreasing the temperature expansion factor of the substrate. The disadvantage is that the use of materials other than the traditional epoxy material could increase the sensor cost, thus losing one of the main advantages of the current design.

The use of embedded high permeability material sheets in the sensor construction could improve the sensitivity and noise. However, using embedded, as opposed to electrodeposited, material for the core structure may also lead to an increased cost.

REFERENCES

[1] *Magnetic Sensors and Magnetometers*, P. Ripka, Ed., Artech House, London, U.K., 2001.

[2] K. W. Na, H. S. Park, D. S. Shim, J. S. Hwang, and S. O. Choi, "MEMS-based fluxgate microsensor for digital compass systems," in *Proc. Eurosensors XVII*, 2003, pp. 653–654.

[3] K. Kuchenbrandt, D. Huhnke, K. Lauckner, and M. Schilling, "Preparation and properties of micro-fabricated fluxgate sensors," in *Proc. Eurosensors XVI*, Prague, Czech Republic, 2002, pp. 587–588.

[4] L. Chiesi, P. Kejik, B. Janossy, and R. S. Popovic, "CMOS planar 2D micro-fluxgate sensor," *Sens. Actuators A*, vol. 82, no. 1-30, pp. 174–180, 2000.

[5] P. Kejik, L. Chiesi, B. Janossy, and R. S. Popovic, "CMOS a new compact 2D planar fluxgate sensor with amorphous metal core," *Sens. Actuators A*, vol. 81, pp. 180–183, 2000.

[6] R. P. Almazán, L. Perez, C. Aroca, M. C. Sánchez, E. López, and P. Sánchez, "Magnetometric sensor based on planar spiral coils," *J. Magn. Magn. Mater.*, vol. 254–255 C, pp. 630–632, 2002.

[7] O. Dezuari, E. Belloy, S. E. Gilbert, and M. A. M. Gijs, "Printed circuit board integrated fluxgate sensor," *Sens. Actuators A*, vol. 81, pp. 200–203, 2000.

[8] E. Belloy, S. E. Gilbert, O. Dezuari, M. Sancho, and M. A. M. Gijs, "A hybrid technology for miniaturised inductive device applications," *Sens. Actuators A*, vol. 85, pp. 304–309, 2000.

[9] O. Dezuari, S. E. Gilbert, E. Belloy, and M. A. M. Gijs, "Development of a novel printed circuit board technology for inductive device applications," *Sens. Actuators A*, vol. 76, pp. 349–355, 1999.

[10] P. D. Dimitropoulos, J. N. Avaritsiotis, and E. Hristoforou, "A novel micro-fluxgate sensor based on the AMR effect of ferromagnetic film-resistors," *Sens. Actuators A*, vol. 107, pp. 238–247, 2003.

[11] S. O'Reilly *et al.*, "New integrated planar magnetic cores for inductors and transformers fabricated in MCM-L technology," in *Proc. IMAPS-US*, Chicago, IL, Oct. 1999, pp. 493–498.

[12] A. Tipek, P. Ripka, T. O'Donnell, and J. Kubik, "PCB technology used in fluxgate sensor construction," in *Proc. Eurosensors XVII*, 2003, pp. 424–425.

[13] P. Ripka, J. Kubik, M. Duffy, W. G. Hurley, and S. O'Reilly, "Current sensor in PCB technology," in *Proc. IEEE Sensors Conf.*, 2002, pp. 779–784.

[14] P. Ripka, S. O. Choi, A. Tipek, S. Kawahito, and M. Ishida, "Pulse excitation of the micro-fluxgate sensors," *IEEE Trans. Magn.*, vol. 37, no. 4, pp. 1998–2000, Apr. 2001.

[15] A. Tipek, P. Kašpar, A. Platil, and A. Cerman, "Magnetic sensors and their temperature testing," *J. Elect. Eng.*, vol. 53, no. 10/s, pp. 56–58, 2002.

Alois Tipek received the Engineering degree and the M.S. and Ph.D. degrees (in fluxgate sensors, fluxgate magnetometers, and their testing and calibration) from the Czech Technical University, Prague, Czech Republic, in 1999 and 2003, respectively.

He participated in several Czech research projects, including the 1998 biomedical application of fluxgate magnetometers, the 1999 satellite fluxgate magnetometer, and the 2001 micro-fluxgate sensors testing. He is currently a Postdoctoral fellow within the Embark Initiative fellowship working in the Tyndall National Institute (former NMRC), Cork, Ireland. His fellowship is focused on the design, fabrication, and characterization of electromagnetic based micro switches.

Dr. Tipek received the "SIEMENS—2002" award for Ph.D. students.

Terence O'Donnell (M'96) received the B.E. degree in electrical engineering and the Ph.D degree for research in the area of finite element analysis of magnetic field problems from University College, Dublin, Ireland, in 1991 and 1996, respectively.

He is presently a Senior Research Officer with the Tyndall National Institute (former NMRC), Cork, Ireland, where he is currently leading the team researching integrated magnetics. He has worked on numerous research projects relating to the design, modeling, and fabrication of planar magnetics for power conversion and data communications, integrated RF inductors, magnetic field sensors, and magnetics for remote inductive powering. His current research interests include the design, modeling, and fabrication of integrated magnetic components.

Pavel Ripka (M'76–SM'81–F'87) received the Engineering degree, the C.Sc. degree (equivalent to the Ph.D. degree), the Docent degree, and the Professor degree from the Czech Technical University (CTU), Prague, Czech Republic, in 1984, 1989, 1996, and 2002, respectively.

From 1991 to 1993, he was a Visiting Researcher with the Danish Technical University and, during 2001, he held the Marie Curie Experienced Researcher's Fellowship at the National University of Ireland, Galway. He is currently with the Department of Measurement, Faculty of Electrical Engineering, CTU, as a Professor, lecturing in measurement, engineering magnetism, and sensors. His main research interests are magnetic measurements and magnetic sensors, especially fluxgates.

He is a member of the Elektra society, the Czech Metrological Society, the Czech National IMEKO Committee, the Eurosensors Steering Committee, and he is an Associate Editor of the IEEE SENSORS JOURNAL. He was a General Chairman of the Eurosensors XVI Conference, Prague, 2002.

Jan Kubik received the Engineering degree from the Czech Technical University, Prague, Czech Republic, in 2003, where he is currently pursuing the Ph.D. degree in the Department of Measurement.

His research interests are in magnetic sensors (AMR, GMR, and fluxgate) and computer-controlled testing systems.